Hindawi Publishing Corporation
EURASIP Journal on Wireless Communications and Networking
Volume 2009, Article ID 516837, 7 pages
doi:10.1155/2009/516837

Research Article

A TR-UWB Downconversion Autocorrelation Receiver for Wireless Body Area Network

S. M. Riazul Islam, Sana Ullah, Md. Humaun Kabir, M. A. Ameen, and Kyung Sup Kwak

Telecommunication Engineering Research Laboratory, Inha University, Incheon, 402-751, South Korea

Correspondence should be addressed to S. M. Riazul Islam, riazuldu@yahoo.com

Received 20 March 2009; Revised 21 May 2009; Accepted 21 July 2009

Recommended by Chia-Chin Chong

Low power UWB receiver architecture is proposed for a Wireless Body Area Network (WBAN). This receiving technology is a synergy of existing downconversion-based narrowband rejection mechanism in RF front end and signal processing in frequency domain. Frequency components of converted and filtered UWB pulses are separated into real and imaginary parts, independently correlated and effectively combined to achieve an improved output Signal to noise ratio (SNR). An extensive mathematical analysis has been performed to formulate the close-form expressions for SNRs in order to compare system performances toward favorable BER under BPSK modulation scheme. Analysis shows that optimal rotation of coordination plays an important role for the enhancement of receiving SNR which is further confirmed by computer simulation. A wide range of link level simulation (LLS) urges that the proposed system is more power efficient in higher-order modulation (HOM) schemes. Transmitted Reference (TR) scheme has been considered as the basis for wideband communication.

1. Introduction

Cardiovascular disease is the leading cause of death [1–4] and it accounts for approximately 30% of all deaths worldwide [5] requiring giant healthcare expenditure [6]. A Wireless Body Area Network (WBAN) allows the integration of intelligent, miniaturized, low-power, invasive, and noninvasive sensor nodes to monitor body function and the surrounding environment [7]. Each intelligent node has enough capability to process and forward information to a base station for diagnosis and prescription. A WBAN provides long-term health monitoring of patients under natural physiological states without constraining their normal activities. It can be used to develop a smart and affordable health care system and can be part of diagnostic procedure, maintenance of chronic condition, supervised recovery from a surgical procedure, and handling emergency events. One of the major components of WBAN is low-power miniaturized sensor [7]. This paper aims to develop an extremely low power receiver that can be employed for WBAN.

On the other hand, Ultra-WideBand (UWB) technology has gained much attention during the last few years as a potential candidte for future wireless short-range data communication. Federal Comunications Commission (FCC) has already alocated the spectrum from 3.1 GHz to 10.6 GHz for UWB applications. Due to its large bandwidth, UWB has the promise of high data rates [8]. A particular type of UWB communication is impulse radio [9], where very short transient pulses are transmitted rather than a modulated carrier. Consequently, the spectrum is spread over several GHz, complying with the definition of UWB. Currently, the rake receiver is considered to be a very promising candidate for UWB reception, due to its capability of collecting multipath components [10]. However, perfect synchronization can never be accomplished. Another issue is the matching of the template with the received pulse. Moreover, often a lot of rake fingers are required to accommodate the wireless channel, rendering it riot favorable from an implementation point of view. Indeed, low complexity rake receivers are being investigated in [11]. The Transmitted Reference (TR) scheme proposed by Hoctor and Tamlinson in [12] does not suffer from the aforementioned problems and requires fewer RF building blocks compared to the multiple finger rake receiver. The core part of the transmitted reference scheme

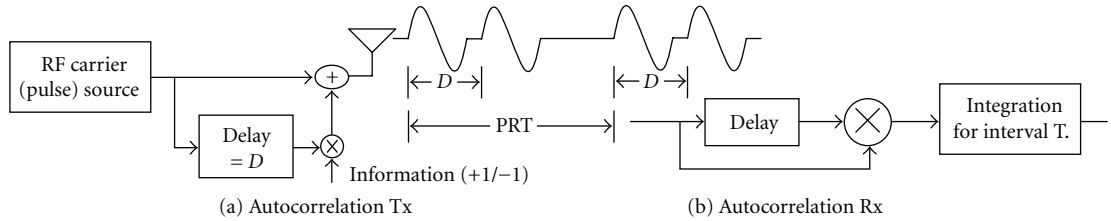

Figure 1: Autocorrelation Transceiver: (a) Transmitter, (b) Receiver.

receiver, alternatively known as "autocorrelation receiver," is shown in Figure 1. This figure shows that TR scheme may be implemented by transmitting pair of identical pulses (called doublets) separated by a time interval D, known to both receiver and transmitter.

The transmitted data is encoded by relative phases of two pulses. The first pulse acts as a reference and the second pulse is the modulated one. The receiver delays the first pulse by the delay D, multiplies it with the second pulse, and integrates the result over one delay length, which in fact correlates the two pulses. When using polar Non Return to Zero (NRZ) modulation, for a logical zero, a pulse is transmitted, subsequently followed by a polarity reversed pulse. To send a logical one, two pulses with the same polarity are sent sequentially. The absolute value of the output after integration is in fact the energy of the pulse while the polarity of the output contains the data. If the output is negative, this corresponds to a logical zero, while a positive output corresponds to a logical one. Thus, the information is in the relative polarity of the two pulses and the delay between them acts as a synchronization mechanism. As long as the two consecutive pulses have corresponding waveforms except for their polarity, the autocorrelation receiver can detect them properly. Yet, directly processing at UWB frequencies, due to the inherent influence of on-chip parasitic reactances at these frequencies, requires relatively large currents, or the use of expensive high speed technologies (SiGe, GaAr).

The work in [13] suggests a new receiver architecture based on the TR scheme [12] for its mentioned advantages with the rake receiver. It deals with interference rejection by filtering and avoids high frequency on-chip processing by using frequency conversion. Frequency conversion in this receiver is done differently from the traditional narrowband system to reject narrowband interference by making a proper choice for the frequency of the local oscillator (LO). The authors in [13] show a lot of advantages of their proposed UWB receiver. For example, it does not suffer from timing and template matching problems, and it circumvents processing at high frequencies, thereby reducing the on-chip circuit complexity and power consumption. Recently, many works have been done to digitally implement the TR-UWB system. However, the limited speed and resolution of the current ADC technology have been a major drawback. To lessen the constraints in ADC sampling speed required for digitally implementing the TR-UWB system, a technique using signal expansions into frequency components has been proposed in [14]. Application of proposed technique in [14] on the receiver architecture suggested in [13] may develop a new receiving technology in which the front end is for downconversion-based narrowband rejection and there after, signal processing is carried out in frequency domain. In fact, this is the main idea of our work.

In this article, we develop a new receiver architecture based on transmit reference scheme [12]. It deals with interference rejection by filtering and avoids high-frequency on-chip processing by using frequency conversion. Moreover, this scheme requires very low power compared to the conventional receiver to achieve target signal-to-noise ratio (SNR) so as to make suitable for WBAN and is accomplished by separating frequency components of converted and filtered UWB pulses into real and imaginary parts, independently correlating and effectively combing them. Figure 2 shows a functional diagram for our proposed receiver architecture.

The authors in [15] are dealing with a similar problem where they estimate the joint response of the analysis filter and the propagation channel independently in each subband. However, it does not consider the coordinate rotation; moreover it uses hybrid filtering as subband filters which reduces the design freedom in the aspect of coexistence issues.

2. Analysis of Proposed System

2.1. Interference Rejection. The proposed architecture employs frequency conversion as done in [13] to coexist with other existing narrowband systems. To achieve this technique, a proper choice for the frequency of the Local Oscillator (LO) is made. Let us investigate this issue in terms of some practical numerical values. If the LO frequency is set to the center frequency of the pulse, which for simplicity is chosen to be in the middle of the band allocated by the FCC for UWB (6.85 GHz), the system acts like a zero IF system and the bandwidth is halved, that is, the band from 3.1 GHz to 10.6 GHz is transformed into a baseband signal from DC to 3.75 GHz. However, the wireless LAN (WLAN) originally residing at around 5.5 GHz is shifted to 1.35 GHz, so it is still in band. Another option is to set the oscillator frequency to this WLAN frequency, such that this interference is shifted to around zero making possible to remove it using a simple high-pass or bandpass filter.

A possible disadvantage is that the downconverted bandwidth of the UWB signal extends up to approximately 5.1 GHz and the converted 2.4 GHz interferer falls in band. A third option is to set the LO to 5.5 GHz and filter out below

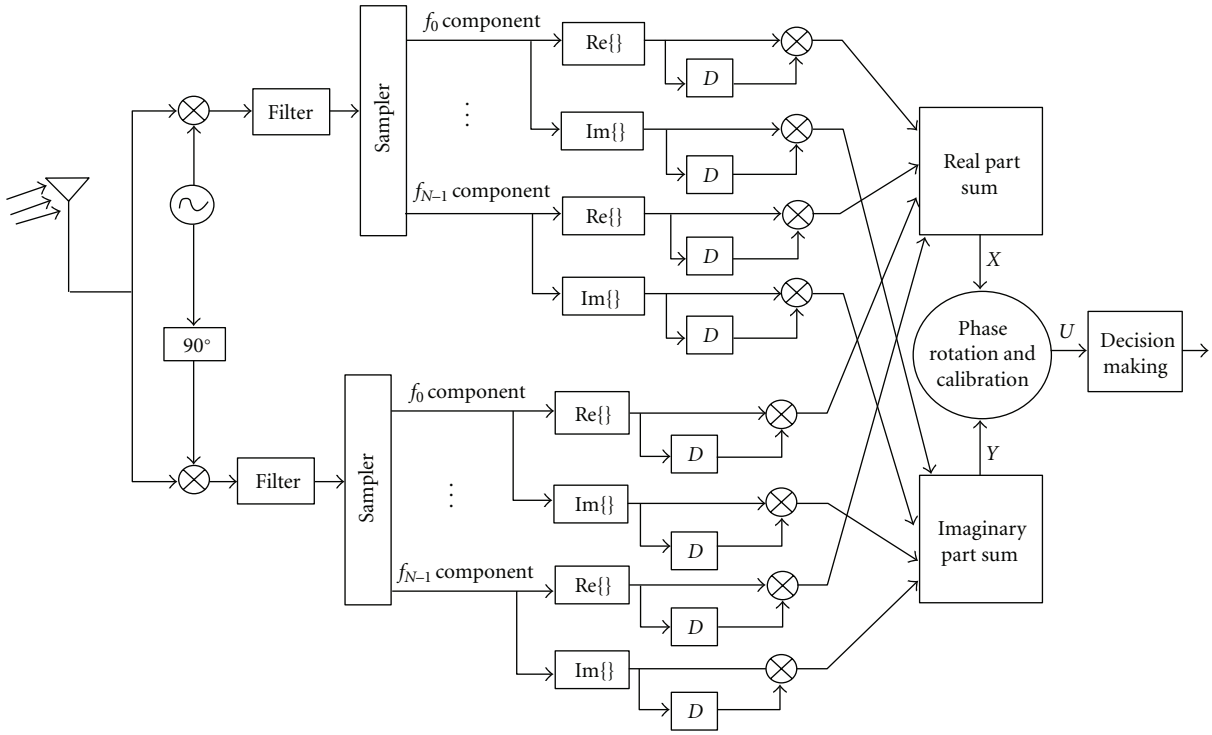

Figure 2: TR-UWB downconversion autocorrelation receiver for WBAN.

$(5.5 - 5.15 =)$ 0.35 GHz and above $(5.5 - 2.4 =)$ 3.1 GHz. By this way, we remove the interferences completely with a simple bandpass filter, albeit at the expense of the loss of part of the incoming frequency band, from $(5.5 + (5.5 \sim 2.4)) =$ 8.6 GHz to 10.6 GHz and from 5.15 to 5.85 GHz, which is a bandwidth of 2.7 GHz, being only 36% or equivalently 1.9 dB.

2.2. Information Decoding and Performance Analysis

Upper Path. First pulse (reference pulse): after mixing with a cosine of angular frequency f_{osc} and normalized amplitude of one, we obtain

$$g(t)\cos(2\pi f_{\text{osc}}t) = A(t)\cos(2\pi f_c t) * \cos(2\pi f_{\text{osc}}t), \quad (1)$$

where, $g(t)$, $A(t)$, f_c are pulse shape (real part of morlet), envelope amplitude and carrier frequency, respectively.

Assuming ideal low-pass filter using $\cos(a)\cos(b) = 1/2[\cos(a+b)+\cos(a-b)]$, the signal after filtering becomes

$$\frac{A(t)}{2}\cos((2\pi f_c - 2\pi f_{\text{osc}})t), \quad (2)$$

after delaying first pulse in the delayed path

$$\frac{A(t-D)}{2}\cos((2\pi f_c - 2\pi f_{\text{osc}})(t-D)). \quad (3)$$

For the second pulse, which will be used as data pulse, the same analysis holds but the input is now a pulse delayed by D in the transmitter:

$$g(t-D)\cos(2\pi f_{\text{osc}}t) = A(t-D)\cos(2\pi f_c(t-D)) * \cos(2\pi f_{\text{osc}}t). \quad (4)$$

The signal after low-pass filter equals

$$\frac{A(t-D)}{2}\cos(2\pi f_c(t-D) - 2\pi f_{\text{osc}}t). \quad (5)$$

Lower Path. Following the same calculation process after delaying first pulse in the delayed path:

$$-\frac{A(t-D)}{2}\sin((2\pi f_c - 2\pi f_{\text{osc}})(t-D)), \quad (6)$$

the second pulse after low-pass filter equals

$$-\frac{A(t-D)}{2}\sin(2\pi f_c(t-D) - 2\pi f_{\text{osc}}t). \quad (7)$$

Terms in (5) and (7) yield the correlator's outputs in the upper path and lower path, respectively. Let us represent these outputs in terms of data pulse $(g_D(t))$ and its delayed version $(g_R(t-D))$ and hence (5) or (7) integrated over sample time can be written as

$$z = \int g_R(t-D)g_D(t)dt, \quad (8)$$

z can be thought as the correlator output under noise free channel.

Using Parseval's theorem, (8) can be rewritten as

$$z = \int g_S(t) g_D^*(t) dt = \int G_S(f) G_D^*(f) df, \tag{9}$$

where, $g_D(t)$ and $g_S(t)$ are data pulse and D-delayed reference pulse, respectively.

To implement the right most term in (9), we need the frequency components of $G_S(f)$ and $G_D^*(f)$ at discrete position of frequency domain. This is realized by a series of analog correlators and termed as sampler in Figure 2. Due to Fourier transform properties, the frequency resolution Δf achievable from a time-domain signal confined in T duration is calculated by $\Delta f = 1/T$. Thus, the sample values of $G_S(f)$ and $G_D^*(f)$ at discrete position $f = f_n$ $(n = 0, \ldots, N-1)$ can be obtained from the sampler.

However, (9) can be written in terms of information bit represented by d_i,:

$$z = d_i \int |G_S(t)|^2 df. \tag{10}$$

Under AWGN, a frequency component of a D-delayed reference pulse at $f = f_n, r_{S,n}$, can be expressed as

$$r_{S,n} = a_{S,n} + jb_{S,n} + p_{S,n} + jq_{S,n}, \tag{11}$$

where $G_{S,n}(f_n) = a_{S,n} + jb_{S,n}$ is a signal component, and $p_{S,n} + jq_{S,n}$ is a noise component.

The frequency component of a data pulse at $f = f_n, r_{D,n}$ can likewise be expressed as

$$r_{D,n} = a_{D,n} + jb_{D,n} + p_{D,n} + jq_{D,n}, \tag{12}$$

where $G_{D,n}(f_n) = a_{D,n} + jb_{D,n}$ is a signal component and $p_{D,n} + jq_{D,n}$ is noise.

A discrete form for (8) is

$$z = \sum_n r_{S,n} r_{D,n}^*. \tag{13}$$

According to (10), a signal signature resides only on real-axis. Thus a receiver to implement (13) uses the following decision rule:

$$\hat{d} = \begin{cases} 1 & \text{for } \mathrm{Re}\{z\} > 0, \\ -1 & \text{for } \mathrm{Re}\{z\} < 0. \end{cases} \tag{14}$$

Let us investigate the term $\mathrm{Re}\{z\}$ in detail. $\mathrm{Re}\{z\}$, for *upper path*, can be manipulated as

$$\begin{aligned} \mathrm{Re}^u\{z\} &= \sum_n \mathrm{Re}\left\{r_{S,n} r_{D,n}^*\right\} \\ &= \sum_n \mathrm{Re}\{r_{S,n}\}\,\mathrm{Re}\{r_{D,n}\} + \sum_n \mathrm{Im}\{r_{S,n}\}\,\mathrm{Im}\{r_{D,n}\} \end{aligned} \tag{15}$$

$\mathrm{Re}^u\{z\} = \sum_n \mathrm{Re}\{r_{S,n} r_{D,n}^*\}$ in (15) can be rewritten as $\mathrm{Re}^u\{z\} = \sum_n \mathrm{Re}\{r_{S,n} r_{D,n}^*\} = \alpha^u + \omega_x^u$, where $\alpha^u = \sum_n a_{S,n} a_{D,n}$ which comes from the real part of signal components and $\omega_x^u = \sum_n (a_{S,n} p_{D,n} + p_{S,n} a_{D,n} + p_{S,n} p_{D,n})$.

In the same manner, $\sum_n \mathrm{Im}\{r_{S,n}\}\mathrm{Im}\{r_{D,n}\} = \beta^u + \omega_y^u$, where $\beta^u = \sum_n b_{S,n} b_{D,n}$ and $\omega_y^u = \sum_n (b_{S,n} q_{D,n} + q_{S,n} b_{D,n} + q_{S,n} q_{D,n})$.

In the same way, for *lower path*,

$$\begin{aligned} \mathrm{Re}^l\{z\} &= \sum_n \mathrm{Re}\left\{r_{S,n} r_{D,n}^*\right\} \\ &= \sum_n \mathrm{Re}\{r_{S,n}\}\,\mathrm{Re}\{r_{D,n}\} + \sum_n \mathrm{Im}\{r_{S,n}\}\,\mathrm{Im}\{r_{D,n}\} \end{aligned} \tag{16}$$

$\mathrm{Re}^l\{z\} = \sum_n \mathrm{Re}\{r_{S,n} r_{D,n}^*\}$ in (16) can be rewritten as $\mathrm{Re}^l\{z\} = \sum_n \mathrm{Re}\{r_{S,n} r_{D,n}^*\} = \alpha^l + \omega_x^l$, where $\alpha^l = \sum_n c_{S,n} d_{D,n}$, which comes from the real part of signal components and $\omega_x^l = \sum_n (c_{S,n} k_{D,n} + k_{S,n} c_{D,n} + k_{S,n} k_{D,n})$.

In the same manner, $\sum_n \mathrm{Im}\{r_{S,n}\}\mathrm{Im}\{r_{D,n}\} = \beta^l + \omega_y^l$, where $\beta^l = \sum_n d_{S,n} d_{D,n}$ and $\omega_y^l = \sum_n (d_{S,n} l_{D,n} + l_{S,n} d_{D,n} + l_{S,n} l_{D,n})$.

Thus, combining (15) and (16), we get

$$\mathrm{Re}\{z\} = \alpha + \beta + \omega_x + \omega_y, \tag{17}$$

where $\alpha = \alpha^u + \alpha^l$, $\beta = \beta^u + \beta^l$; $\omega_x = \omega_x^u + \omega_x^l$, $\omega_y = \omega_y^u + \omega_y^l$.

Two random variables w_x and w_y are zero mean and independent each other, so the mean and variance of $\mathrm{Re}\{z\}$ are

$$\begin{aligned} E[\mathrm{Re}\{z\}] &= \alpha + \beta, \\ \mathrm{var}[\mathrm{Re}\{z\}] &= E\left[(w_x + w_y)^2\right] = V_x + V_y. \end{aligned} \tag{18}$$

Thus, the resultant SNR at the correlator output is

$$\mathrm{SNR}_A = \frac{(\alpha + \beta)^2}{V_x + V_y}, \tag{19}$$

and its BER performance is

$$\mathrm{BER}_A = \frac{1}{2}\mathrm{erfc}\left(\sqrt{\frac{\mathrm{SNR}_A}{2}}\right). \tag{20}$$

Defining $X = \alpha + w_x$ and $Y = \beta + w_y$. Now a message point for $d_i = 1$ is located at (α, β) in the constellation diagram while a message point for $d_i = -1$ is at $(-\alpha, -\beta)$ and hence a decision boundary is the line to bisect the line at right angle connecting two message points. Two message points are always symmetrical with respect to origin, and the connecting line has a slope of $\theta = \tan^{-1}(\beta/\alpha)$. Let us rotate the coordination by θ, then two message points are relocated at $(\alpha_1, 0)$ and $(0, \beta_1)$ where $\alpha_1 = \alpha\cos\theta + \beta\sin\theta$. Then the decision rule becomes

$$\hat{d}_i = \begin{cases} 1 & \text{for } U > 0, \\ -1 & \text{for } U < 0, \end{cases} \tag{21}$$

where $U = X\cos\theta + Y\sin\theta$.

Mean and Variance of U:

$$\begin{aligned} E[U] &= \alpha\cos\theta + \beta\sin\theta = \sqrt{\alpha^2 + \beta^2}, \\ \mathrm{var}[U] &= E[wx\cos\theta + wy\sin\theta] = V_x\cos^2\theta + V_y\sin^2\theta. \end{aligned} \tag{22}$$

Table 1: Simulation parameters.

Parameter	Specifications
Channel model	S4-CM3
Pulse Shape	Gausian 2nd pulse
Over sampling rate	4
Number of frequency components	8
Modulation	BPSK, QPSK, QAM
Number of input data bits	30,000
Filter order	40
Delay	5 samples

So, SNR of new system

$$\mathrm{SNR}_B = \frac{\alpha^2 + \beta^2}{V_x \cos^2\theta + V_y \sin^2\theta}, \tag{23}$$

and BER

$$\mathrm{BER}_B = \frac{1}{2}\mathrm{erfc}\left(\sqrt{\frac{\mathrm{SNR}_B}{2}}\right). \tag{24}$$

The ratio of SNRs of two systems is

$$\gamma = \frac{\mathrm{SNR}_B}{\mathrm{SNR}_A} = \frac{Vx + Vy}{(1 + \sin 2\theta)\left(V_x \cos^2\theta + v_y \sin^2\theta\right)}. \tag{25}$$

However, (24) implies that the more θ is departed away from 45°, the better the performance of our proposed receiver architecture. Theoretically, two systems are identical regarding performance when $\theta = 45°$. Suppose that as it is intuitionally, the variance of w_x and w_y are same, then $\gamma = 2$ yielding a reasonable improvement (double or 3 dB) in SNR performance by new system. Similar approaches can be carried out for other modulation schemes such as QPSK and QAM.

3. Simulation and Results

Computer simulation has been performed to evaluate the system performances and we used MATLAB as simulation software. Channel modeling is an important factor to simulate a communication system. As we have used only AWGN channel in our analysis so a corresponding channel model is S4-CM3 (body surface to body surface, LOS) proposed in [16]. As CM3 involves different carrier frequency/bands, the choice of LO is dynamic. A detailed of simulation parameters is listed in Table 1.

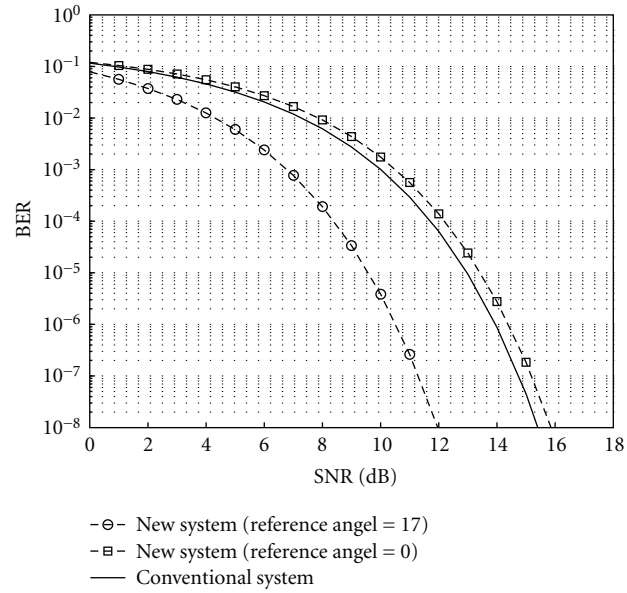

Figure 3: Performance Comparison between New System and Conventional System (BPSK Scheme).

Now let us evaluate the system in terms of its performances. Figure 3 proves that our theoretical analysis is accurate as it shows 3 dB SNR improvement by new system for reference angle 17° (same as in [14]) while the performance is almost same for 0° reference.

In addition the proof of our theoretical conclusion we have done an extensive simulation for higher-order adaptive modulation such as QPSK and QAM. Figure 4 shows the scattered noisy signals from which the digital information has been reproduced. Figure 5 indicates that our proposed system is really the novel one as it does 6 dB SNR improvements in every modulation scheme.

4. Conclusions

New low power TR-UWB receiver architecture has been introduced. It amalgams existing downconversion-based narrowband rejection mechanism in RF front end and signal processing in frequency domain. A detailed mathematical framework has been formulated for close form expression of SNR that is used to compare the system performance. Theoretical analysis shows that separating the converted UWB pulses into real and imaginary parts, independently correlating and introducing rotation of coordination brings a 3 dB improvement in performance regarding Signal-to-noise-ratio (SNR) using binary modulation. This theoretical conclusion has been verified by performing computer simulation. Additional link level simulations show that the proposed system is also well behaved for higher order adaptive modulation (HOM) by improving 6 dB SNR in every scheme which is really fruitful for WBAN as it requires extremely low power.

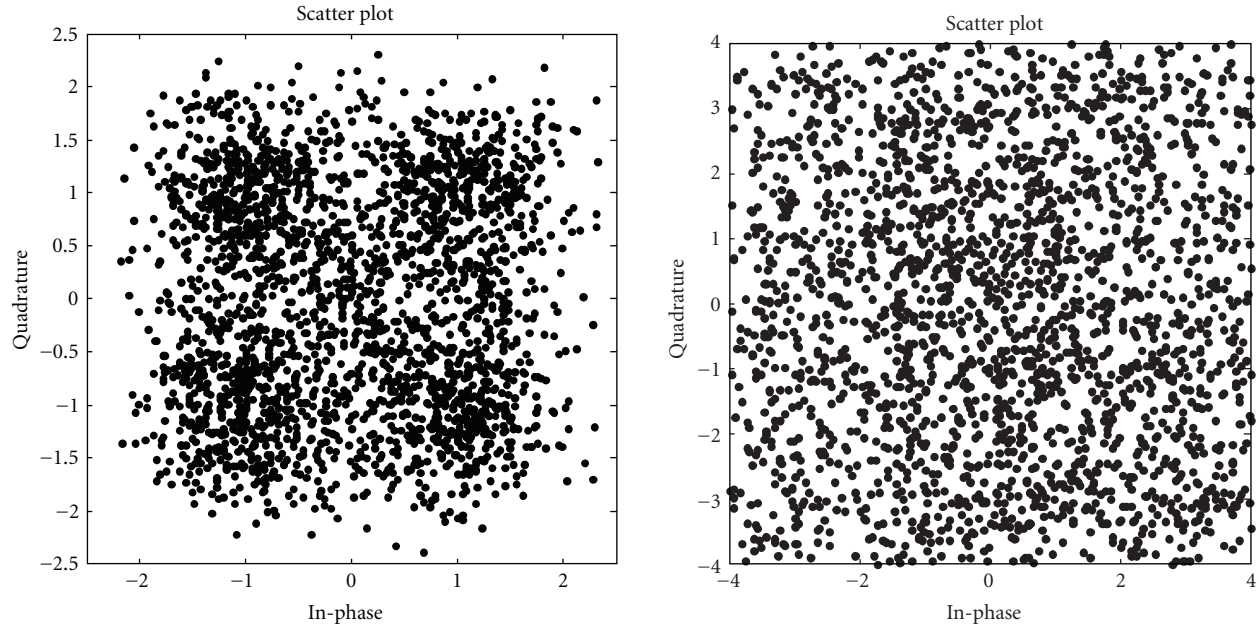

Figure 4: Constellations of noisy signals (first 2500 samples) (QPSK & 16-QAM). BPSK is not included as it is readily realizable. 64-QAM is not given as it appears as if everywhere.

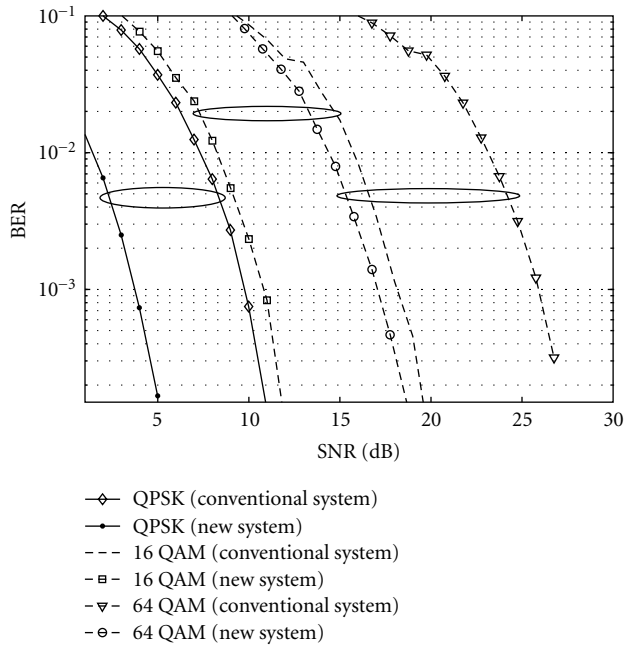

Figure 5: Performance of TR-UWB Downconversion Autocorrelation Receiver (Higher-Order Adaptive Modulation) (reference angle 20° found from simulation indicating the best BER response).

This receiver needs perfect tuning while decomposing the received signal to multiple frequency tones within sampler, otherwise, it suffers from interferences and may creates a number of complexities. In future, the performance of this receiver will be investigated introducing synchronization mechanism. Performance evaluation of this proposed system considering fading environments is also a part of our future work.

References

[1] S. Ullah, S. M. R. Islam, A. Nessa, Y. Zhong, and K. S. Kwak, "Performance analysis of preamble based TDMA protocol for wireless body area network," *Journal of Communication Software and Systems*, vol. 4, no. 3, 2008.

[2] http://www.who.int/whosis/mort/profiles/mort_wpro_kor_repofkorea.pdf, February 2008.

[3] A. Barroso, J. Benson, T. Murphy, et al., "The DSYS25 sensor platform," in *Proceedings of the 2nd International Conference on Embedded Networked Sensor Systems (SenSys '04)*, p. 314, 2004.

[4] B. Lo and G. Z. Yang, "Key technical challenges and current implementations of body sensor networks," in *Proceedings of the 2nd IEEE International Workshop on Body Sensor Networks (BSN '05)*, pp. 1–5, April 2005.

[5] http://www.innovationmagazine.com/innovation/volumes/v7n3/feature2.shtml, March 2008.

[6] C. Borger, S. Smith, C. Truffer, et al., "Health spending projections through 2015: changes on the horizon," *Health Affairs Web Exclusive*, vol. 25, no. 2, pp. 61–73, 2006.

[7] S. Ullah, H Higgins, and K. S. Kwak, "A study of implanted and wearable BSN," in *Agent and Multi-Agent Systems: Technologies and Applications*, vol. 4953 of *Lecture Notes in Computer Science*, pp. 464–473, Springer, Heidelberg, Germany, 2008.

[8] J. Foerster, E. Green, S. Somayazulu, and D. Leeper, "Ultra-wideband technology for short- or medium-range wireless communications," *Intel Technology Journal Q2*, 2001.

[9] M. Z. Win and R. A. Scholtz, "Impulse radio: how it works," *IEEE Communications Letters*, vol. 2, no. 2, pp. 36–38, 1998.

[10] J. G. Proakis, *Digital Communications*, McGraw-Hill, New York, NY, USA, 3rd edition, 1995.

[11] D. Cassioli, M. Z. Win, F. Vatalaro, and A. F. Molisch, "Performance of low-complexity Rake reception in a realistic UWB channel," in *Proceedings of the IEEE International Conference on Communications (ICC '02)*, vol. 2, pp. 763–767, New York, NY, USA, May 2002.

[12] R. T. Hoctor and H. W. Tomlinson, "Dday-hopped transmitted-reference RF communications," in *Proceedings of the IEEE Conference on Ultra Wideband System and Technologies*, pp. 265–270, May 2002.

[13] S. Lee, S. Bagga, and W. A. Serdijn, "A quadrature downconversion autocorrelation receiver architecture for UWB," in *Proceedings of the Conference on Ultra Wideband Systems and Technologies (UWBST '04)*, pp. 6–10, May 2004.

[14] S. Woo, H. Yang, S. Yang, Y. Kim, J. Yook, and B. Kang, "A new TR-UWB receiver exploiting frequency components," *IEICE Transactions on Communications*, vol. E91-B, no. 5, pp. 1608–1611, 2008.

[15] L. Feng and W. Namgoong, "An oversampled channelized UWB receiver with transmitted reference modulation," *IEEE Transactions on Wireless Communications*, vol. 5, no. 6, pp. 1497–1505, 2006.

[16] A. Austrin, "Channel Model for WBAN," IEEE P802.15 Working Group for Wireless Personal Area Networks (WPAN), P802.15-08-0780-06-0006, March 2009.